Slender elastic filaments sedimenting through low-Reynolds number flows

Ron Shvartsman

PACM independent work
Princeton University
Spring 2025
Advisor: Professor Howard Stone

This paper represents my work in accordance with University regulations.

/s/ Ron Shvartsman

1 Introduction

In this paper, I will describe my research under the supervision of Professor Howard Stone and Dr. Rodolfo Brandão in Summer 2023, on the sedimentation of a slender elastic filament in a low Reynolds number fluid. This problem was considered in a classical paper by Xu and Nadim in 1994 [1], where they linearized the equations of elasticity and used resistive force theory to find a unique deflection profile that looks like a "U" shape.

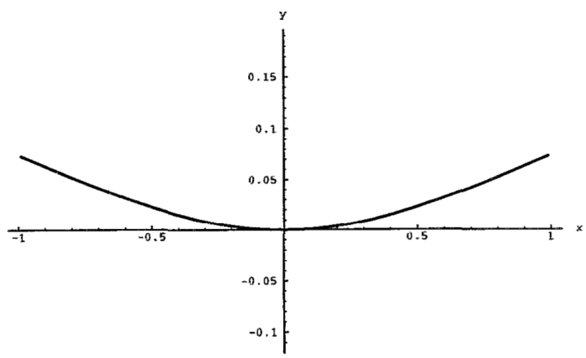

Figure 1: Deflection profile found in [1]

However, a numerical study by Lagomarsino et.al. in 2005 [2] that modeled the filament as a series of beads found additional "W"-like shapes in the limit that the filament was highly flexible, contradicting uniqueness of Xu and Nadim's shape. This motivated our work to find deflection profiles as a function of filament flexibility.

2 Problem formulation

2.1 Elastohydrodynamic model

Consider an elastic filament (density ρ_*, bending modulus B_*, length $2\ell_*$, cross-sectional radius a_*) falling under gravity (gravitational acceleration $\mathbf{g}_*$) through a quiescent fluid (viscosity μ_*). The asterisk indicates a dimensional quantity. Our focus is on steady states, where the deformable filament translates at a constant velocity $\mathbf{U}_*$. We assume that the centerline of the filament

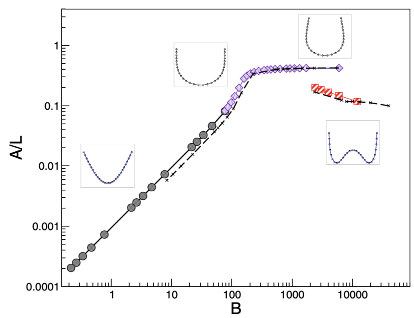

Figure 2: Plot of bending amplitude (displacement at the end of the filament) as a function of B, a dimensionless measure of flexibility. In the small B limit, the shape recovers the Xu and Nadim solution, but at large B the solution becomes nonunique and a novel "W" shape appears.

is planar and symmetric about a line passing through its midpoint in the direction of $\mathbf{g}_*$ (see Fig. 3); these symmetry conditions directly imply that $\mathbf{U}_*$ and $\mathbf{g}_*$ are collinear.

In accordance with the above assumptions, we introduce Cartesian unit vectors $\{\hat{\mathbf{e}}_x, \hat{\mathbf{e}}_y\}$ and write

$$\mathbf{g}_* = -g_* \hat{\mathbf{e}}_y, \qquad \mathbf{U}_* = -U_* \hat{\mathbf{e}}_y. \tag{1}$$

Adopting a reference frame comoving with the filament, we parameterise the filament centerline by

$$\mathbf{x}_*(s) = x_*(s_*)\hat{\mathbf{e}}_x + y_*(s_*)\hat{\mathbf{e}}_y \tag{2}$$

where s_* is the arc length coordinate measured from the midpoint $-\ell_* \leq s_* \leq \ell_*$; due to the assumed symmetry of the centerline, we can restrict our analysis to half of the filament $0 \leq s_* \leq \ell_*$. The tangent unit vector is

$$\hat{\mathbf{t}} = \frac{d\mathbf{x}_*}{ds_*}, \tag{3}$$

which can be used to define a tangent angle $\theta(s_*)$ via the relation

$$\hat{\mathbf{t}} = \cos\theta\,\hat{\mathbf{e}}_x + \sin\theta\,\hat{\mathbf{e}}_y. \tag{4}$$

In terms of θ, the normal unit vector can be expressed as

$$\hat{\mathbf{n}} = \sin\theta\,\hat{\mathbf{e}}_x - \cos\theta\,\hat{\mathbf{e}}_y, \tag{5}$$

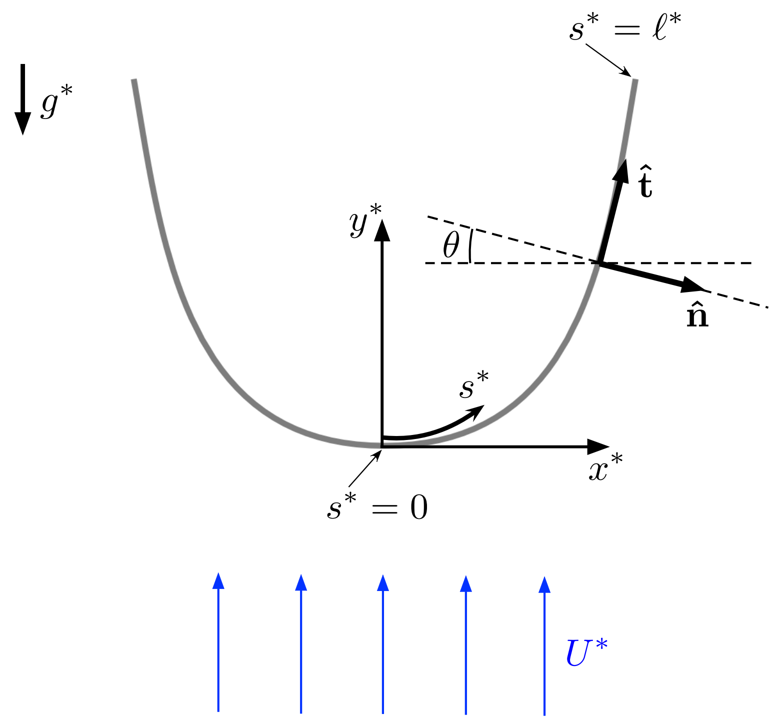

Figure 3: Sketch of the problem setup

and the local curvature as

$$\kappa_* = \frac{d\theta}{ds_*}. \tag{6}$$

Then, we have the familiar relations

$$\frac{d\,\hat{\mathbf{t}}}{ds_*} = -\kappa_*\hat{\mathbf{n}}, \tag{7a}$$

$$\frac{d\,\hat{\mathbf{n}}}{ds_*} = \kappa_*\hat{\mathbf{t}}. \tag{7b}$$

Since the filament is in dynamic equilibrium, its shape is determined by local force and torque balances. The local force balance reads

$$\mathbf{f}_*^{(i)} + \mathbf{f}_*^{(g)} + \mathbf{f}_*^{(h)} = \mathbf{0}, \tag{8}$$

where $\mathbf{f}_*^{(i)}$, $\mathbf{f}_*^{(g)}$ and $\mathbf{f}_*^{(h)}$ are, respectively, the internal, gravitational, and hydrodynamic forces per unit length, which we now describe.. The internal force per unit length can be written as

$$\mathbf{f}_*^{(i)} = \frac{d\mathbf{F}_*}{ds_*}, \tag{9}$$

where

$$\mathbf{F}_* = T_* \ \hat{\mathbf{t}} + N_* \ \hat{\mathbf{n}} \tag{10}$$

is the cross-sectionally averaged internal force. The gravitational force per unit length is

$$\mathbf{f}_*^{(g)} = -\pi a_*^2 \rho_* g_* \hat{\mathbf{e}}_y. \tag{11}$$

To model hydrodynamic effects, we assume that the filament is sufficiently small and slender, such that Resistive Force theory for Stokes flows is applicable, and

$$\mathbf{f}_*^{(h)} = -\frac{4\pi\mu_*}{\ln 1/\epsilon}\left(\frac{1}{2}\hat{\mathbf{t}}\hat{\mathbf{t}} + \hat{\mathbf{n}}\hat{\mathbf{n}}\right) \cdot \mathbf{u}_*, \tag{12}$$

where $\epsilon = a_*/\ell_* \ll 1$ is the aspect ratio of the filament. We note that (12) only depends on the local orientation of the filament relative to the flow; hence, it neglects nonlocal effects, such as those due to the finite size of the filament, whose contribution to the hydrodynamic force are at least a factor of $(\ln 1/\epsilon)^{-1}$ smaller than (12).

Substituting (1) and (9)–(12) into (8) and decomposing the force balance into its tangential and normal components with the aid of (4)–(6), we arrive at the tangential force balance

$$\frac{dT_*}{ds_*} + \kappa_* N_* + \frac{1}{2}\frac{4\pi\mu_* U_*}{\ln 1/\epsilon}\sin\theta - \pi a_*^2 \rho_* g_* \sin\theta = 0, \tag{13}$$

and the normal force balance

$$\frac{dN_*}{ds_*} - \kappa_* T_* + \frac{4\pi\mu_* U_*}{\ln 1/\epsilon}\cos\theta + \pi a_*^2 \rho_* g_* \cos\theta = 0. \tag{14}$$

The torque balance for a planar curve can be written as a single scalar equation,

$$\frac{dM_*}{ds_*} - N_* = 0, \tag{15}$$

where M_* is the internal bending moment in the filament. For an elastic filament with a cylindrical cross-section, the common constitutive description is $M_* = B_*\kappa_*$. Substitution of this relation into (15) furnishes

$$\frac{d\kappa_*}{ds_*} = \frac{N_*}{E_* I_*}. \tag{16}$$

Lastly, we specify the boundary conditions for the problem. At the midpoint ($s_* = 0$), we impose the symmetry conditions

$$\theta(0) = N_*(0) = 0, \tag{17}$$

as well as

$$\mathbf{x}_*(0) = 0, \tag{18}$$

which specifies the origin of the coordinate system. At the end ($s_* = \ell_*$), we impose free-end boundary conditions,

$$T_*(\ell_*) = N_*(\ell_*) = \kappa_*(\ell_*) = 0. \tag{19}$$

2.2 Dimensionless problem

We normalize lengths by ℓ_*, forces by $\pi a_*^2 \rho_* g_* \ell_*$, and velocities by $\frac{\pi a_*^2 \rho_* g_*}{\mu_*} \frac{\ln 1/\epsilon}{4\pi}$. Then, with dimensionless quantities denoted without an asterisk, our model reduces to a system of first-order differential equations,

$$\frac{dT}{ds} + \kappa N = (1 - \frac{1}{2}U)\sin\theta, \tag{20a}$$

$$\frac{dN}{ds} - \kappa T = (U - 1)\cos\theta, \tag{20b}$$

$$\frac{d\kappa}{ds} = \eta N, \tag{20c}$$

$$\frac{d\theta}{ds} = \kappa, \tag{20d}$$

$$\frac{dx}{ds} = \cos\theta, \tag{20e}$$

$$\frac{dy}{ds} = \sin\theta, \tag{20f}$$

defined in the domain $s \in [0, 1]$, corresponding to half of the filament. The problem involves six unknown functions $(T, N, \kappa, \theta, x, y)$ and the unknown speed U; therefore, we impose seven boundary conditions

$$\theta(0) = N(0) = \kappa(1) = N(1) = T(1) = x(0) = y(0) = 0 \tag{21}$$

Importantly, the dimensionless problem depends on a single dimensionless group, which appears in equation (20c),

$$\eta = \frac{\lambda_* g_* \ell_*^3}{E_* I_*}, \tag{22}$$

which we refer to as the compliance of the filament [3]; it corresponds to the ratio of the characteristic gravitational force to the elastic force, and therefore serves as a measure of the flexibility of the filament.

We note that the problem governing T, N, κ, θ and U, given by (20a-d), is uncoupled from the problem governing x and y given by (20e-f). It will be convenient for the subsequent analysis to substitute (20c-d) into (20a-b) to arrive at a problem involving θ, T and U only,

$$\frac{dT}{ds} + \frac{1}{\eta}\frac{d\theta}{ds}\frac{d^2\theta}{ds^2} = \left(1 - \frac{1}{2}U\right)\sin\theta, \tag{23a}$$

$$\frac{1}{\eta}\frac{d^3\theta}{ds^3} - \frac{d\theta}{ds}T = (U-1)\cos\theta, \tag{23b}$$

with boundary conditions

$$\theta(0) = 0, \qquad \frac{d^2\theta}{ds^2}(0) = 0 \tag{24a}$$

$$\frac{d\theta}{ds}(1) = 0, \quad \frac{d^2\theta}{ds^2}(1) = 0, \quad T(1) = 0. \tag{24b}$$

Once the angle θ is determined from the above problem, the shape of the filament can be calculated by straightforward integration of (20e-f).

3 Small deformation solutions

We seek solutions to these equations in the small amplitude limit for small and large compliances: That is, $\theta(s) \ll 1$, $T(s) \ll 1$. This also implies $u - 1 \ll 1$, from (23b). Note that the trivial solution $\theta = T = 0, u = 1$ is always a solution, corresponding to a flat filament. Expanding these unknowns in a general way, we write

$$\theta \sim \delta_\theta \Theta \tag{25a}$$

$$T \sim \delta_T \mathcal{T} \tag{25b}$$

$$u - 1 \sim \delta_u U \tag{25c}$$

where $\delta_\theta, \delta_T, \delta_u$ are functions of η, and $\Theta(s), \mathcal{T}(s), U$ are $\mathcal{O}(1)$ functions or constants independent of η. Furthermore, we assume that derivatives are of the same order as their parent functions.

With this general scaling, noting also that to lowest order, $\sin\theta \sim \delta_\theta \Theta$ and $\cos\theta \sim 1$, (23) and (24) become

$$\delta_T \mathcal{T}_s + \frac{\delta_\theta^2}{\eta}\Theta_s\Theta_{ss} \sim \frac{1}{2}\delta_\theta\Theta \tag{26a}$$

$$\frac{\delta_\theta}{\eta}\Theta_{sss} - \delta_\theta\delta_T\Theta_s\mathcal{T} \sim \delta_u U \tag{26b}$$

$$\Theta(0) = 0, \qquad \Theta_{ss}(0) = 0 \tag{27a}$$

$$\Theta_s(1) = 0, \quad \Theta_{ss}(1) = 0, \quad \mathcal{T}(1) = 0 \tag{27b}$$

Comment: For nontrivial solutions, the nonlinear term in (26b) cannot be subdominant for any η. If it were, (26b) would become

$$\begin{aligned} & \frac{\delta_\theta}{\eta}\Theta_{sss} \sim \delta_u U \\ \implies \quad & \Theta_{sss} \sim U \\ \implies \quad & \Theta \sim \frac{1}{6}Us^3 + c_2 s^2 + c_1 s + c_0 \end{aligned} \tag{28}$$

Then, applying (27), this implies that $\Theta = 0$, which is the trivial solution.

3.1 $\eta \ll 1$ limit

In the limit of small compliances, where the filament is weakly flexible, our system does not support nontrivial solutions. To see this, we note that from the comment above, $\delta_\theta\delta_T\Theta_s\mathcal{T}$ must be dominant in (26b), so we either have $\delta_\theta\delta_T\Theta_s\mathcal{T} \sim \frac{\delta_\theta}{\eta}\Theta_{sss}$ or $\delta_\theta\delta_T\Theta_s\mathcal{T} \gg \frac{\delta_\theta}{\eta}\Theta_{sss}$. If the former is true, we have $\delta_T \sim \frac{1}{\eta}$, and if the latter is true, we have $\delta_T \gg \frac{1}{\eta}$, both of which are inconsistent with (26a) and small deformations.

3.2 $\eta \gg 1$ limit

For large compliances, (26a) simplifies: $\delta_\theta, \frac{1}{\eta} \ll 1$, so

$$\begin{aligned} &\frac{\delta_\theta^2}{\eta}\Theta_s\Theta_{ss} \ll \frac{1}{2}\delta_\theta\Theta \\ &\implies \delta_T\mathcal{T}_s \sim \frac{1}{2}\delta_\theta\Theta \\ &\implies \delta_\theta = \delta_T \end{aligned} \tag{29}$$

Then we can eliminate the angle Θ in (26b) and write (26) as a single equation in the tension and velocity:

$$\frac{\delta_T}{\eta}\,\mathcal{T}_{ssss} - \delta_T^2\,\mathcal{T}_{ss}\mathcal{T} \sim \frac{1}{2}\delta_u\,U \tag{30}$$

Attempting the three term balance, we get the scalings $\delta_\theta = \delta_T = \frac{1}{\eta}, \delta_u = \frac{1}{\eta^2}$, leading to the fourth order BVP

$$\mathcal{T}_{ssss} - \mathcal{T}_{ss}\mathcal{T} \sim \frac{1}{2}\,U \tag{31}$$

with boundary conditions

$$\mathcal{T}_s(0) = 0, \qquad \mathcal{T}_{sss}(0) = 0 \tag{32a}$$

$$\mathcal{T}_{ss}(1) = 0, \quad \mathcal{T}_{sss}(1) = 0, \quad \mathcal{T}(1) = 0 \tag{32b}$$

This is a 4th order nonlinear eigenvalue problem. Dr. Brandão carried out detailed asymptotics in the large $U \gg 1$ limit, but I will not report those results here. This leads to a sequence of eigenvalues that yield the proportionality coefficient in the asymptotic behavior $y(1) \sim \mathcal{O}(\frac{1}{\eta^2}), u \sim \mathcal{O}(\frac{1}{\eta})$.

4 Numerical work

Using numerical pathfollowing with ‘chebfun’ in MATLAB, we can trace out a bifurcation diagram for the velocities or amplitudes of solutions as functions of compliance η. In the large η limit, we can superimpose asymptotic predictions, using the results of Dr. Brandão’s analysis.

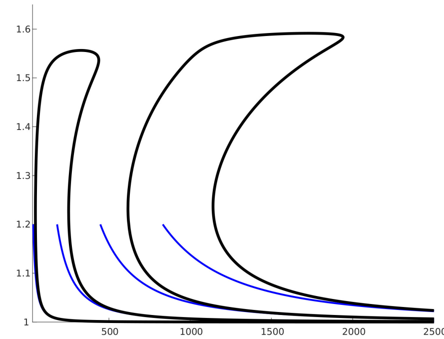

(a) linear scale

Figure 4: velocity bifurcation diagram with asymptotic predictions

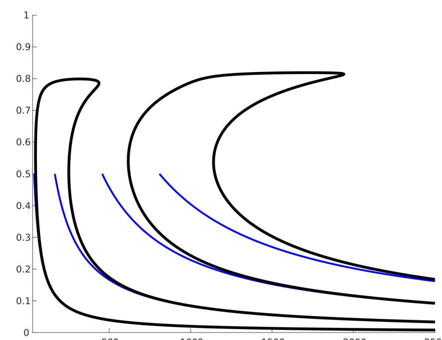

(a) linear scale

Figure 5: amplitude bifurcation diagram with asymptotic predictions

These figures show the characteristic turning point observed in Lagomarsino et.al., which indicates the nonuniqueness of solutions. Since $\eta = B/8$, we observe this point at the same scale as their numerics. However, we can now interpret this in terms of our dimensionless force balance: at large η, a balance exists between all three terms of elasticity, fluid force, and gravity, which is nonlinear through the effects of curvature. Large compliance is precisely the condition that curvature matters, and therefore we expect nonlinearity to play an important role.

5 Conclusion

In this project, we were able to write down a simple model for a complicated problem: one where hydrodynamics, elasticity, and gravity all interact, and where fluid force influence shape and vice versa. The force balance, inspired by Kurzthaler et.al. [3], revealed that in the limit of slender filaments, only the compliance governs the solution to the system. We may also include effects of slenderness, which would lead to a 2 parameter system. This would then reduce to the Xu and Nadim limit as $\eta \to 0$, which is missed in this model.

References

[1] Xianghua Xu and Ali Nadim. Deformation and orientation of an elastic slender body sedimenting in a viscous liquid. *Physics of Fluids*, 6(9):2889–2893, 1994.

[2] M Cosentino Lagomarsino, I Pagonabarraga, and CP Lowe. Hydrodynamic induced deformation and orientation of a microscopic elastic filament. *Physical review letters*, 94(14):148104, 2005.

[3] Christina Kurzthaler, Rodolfo Brandão, Ory Schnitzer, and Howard A Stone. Shape of a tethered filament in various low-reynolds-number flows. *Physical Review Fluids*, 8(1):014101, 2023.